

Analysis of Line Instability in Microgrid by Applying Electrical Power Forecasting Approach

Richard Joseph Mushi¹, Terapong Boonraska², Ashok Paudel¹, Boonruang Marungsri^{1,*}

¹School of Electrical Engineering, Institute of Engineering, Suranaree University of Technology, 111 University Avenue, Muang District, Nakhon Ratchasima 30000, Thailand

²School of Electrical Engineering, Rajamangala University of Technology Rattanakosin, 96 Mu 3 Phutthamonthon Sai 5 Raod, Salaya, Phutthamonthon, Nakhon Pathom 73170, Thailand

*Corresponding author's email: bmshvee@sut.ac.th

Received: 03/12/2019, Accepted: 20/10/2021

Abstract

The line instability and electrical power forecasting are essential techniques for operation control and planning in the microgrid. This paper presents an analysis of the line instability in microgrid by applying the electrical power forecasting approach. A mathematical model of power forecasting was examined using the modified GM (1, 1) model. Besides that, the power flow was represented using a modified IEEE 30 bus test system in MATLAB. Finally, the line instability was analyzed based on the results of power flow, using line stability factor (LQP). The results exhibited that the actual power was close to the power forecasting when the modified GM (1, 1) model combined together with exponential smoothing method. There was a high accuracy of prediction with Mean Absolute Percentage Error (MAPE) less than 1 %. Apart from that, it was cleared shown that the most critical line was 28-27, with a line instability factor of 0.963. The second and third most vital lines were 25-26 and 2-4, having instability factors of 0.759 and 0.568, respectively. For a next day operation and planning in the microgrid, care must be taken by the utility operator to make sure that the microgrid is managed successfully.

Keywords:

Electric Power Forecasting, Microgrid, Power Flow, Line Stability

1. Introduction

The microgrid system includes distributed generation, energy storage system, control devices, and load. The generation sources in the microgrid are made of renewable energy sources and non-renewable energy sources. The renewable energy sources are wind, solar, hydro-power, etc., whereas the non-renewable energy sources are such as coal, petroleum, natural gas, etc.

The microgrid can operate in grid-connected and islanded modes. In this paper, the microgrid is assumed operating in an island model. The power generated by renewable energy sources fluctuated and depends on weather conditions such as wind speed, sunlight, etc. [1], as a result of instability conditions arise in the microgrid. The challenges of instability are the central alarms in microgrid planning and operation control [2]. The main instability problem is a mismatch of power supply and user demands, which leads to voltage instability.

Line instability refers to how far the system is close to voltage flop [3]. The existence of line and voltage instability leads to the voltage collapse and system blackout. Several techniques have been proposed in the literature to analyze line instability. The most four used line stability indexes are; Fast

Voltage Stability Index (FVSI), Line Voltage Stability Index (LVSI), Line Stability Index (Lmn), and Line Stability Factor (LQP) [4].

However, electric power forecasting is a tool to predict upcoming power in a system; this is because understanding the behavior of power in a cutting-edge way is key in operation control, analysis, and planning in microgrid [5]. The power forecasting classified into short-term, medium-term, and long-term forecasting [6]. Short-term forecasting takes duration from hourly to one day even a week, medium-term duration ranges from weekly to monthly, and long-term forecasting is from monthly to yearly. This paper opts to apply short-term forecasting because it is easy to use and requires a small quantity of data to predict the system.

The Grey system is a method that has been widely implemented and studied in many research areas. One of the research areas is the Grey forecasting time-series. According to [7], the Grey forecasting time series uses the Grey differential model (GM) to predict systems. Numerous types of research have been performed using time series prediction, and others tried to modify GM to enhance the accuracy of the prediction model [8]-[10].

1.1 Related Research

Reference [11]-[13] published papers about stability index and voltage collapse prediction without considering application of power forecasting in the network because forecasting determines future state of the system.

This paper presents an analysis of the line instability in microgrid by applying electrical power forecasting. Analysis of electrical power forecasting was carried out using a mathematical of the hybrid model (modified GM (1, 1) and exponential smoothing models) but, the power flow was performed using the IEEE 30 bus standard test system in MATLAB, and finally, the line instability was determined based on power flow results.

2. Methodology

The methodology section gives details of a mathematical model of the modified GM (1, 1), power flow using the Newton-Raphson method, and line instability techniques.

2.1. Build Forecasting Model

Electrical power forecasting is a method applied by the utility to predict future power. In this paper, modified G (1,1) was used together with a simple exponential smoothing method. This is because the GM (1, 1) model is capable in forecasting data which are increased or decreased while, electricity consumptions have a tendency to produce randomly behaviors. Thus, the results obtained from the modified GM (1, 1) model were smoothed in a simple exponential smoothing method. The block diagram of representation of steps from input data to output results is shown in Fig.1.

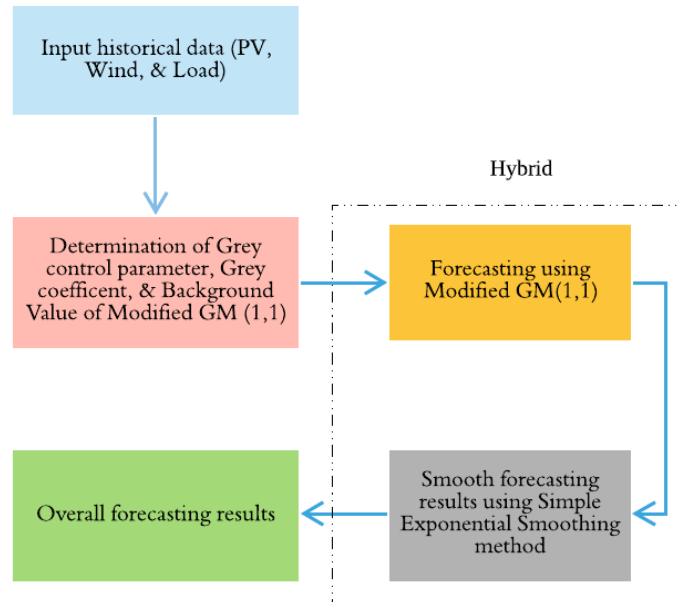


Fig. 1. Build Block for Forecasting Model.

2.1.1 Selection of Model

The GM (1,1) is the mathematical model and selection was made by comparing GM (1,1) against other mathematical models such as regression, ARIMA, and Holt's exponential. The selection of Grey model was based on recommendation proposed by [14]. The criteria set to make comparisons are types of data, duration of forecasting, amount of data needed, and required mathematical skills for evaluating data, as indicated in Table 1.

Table 1 Comparison of Models for Forecasting [14] cited in [15].

Prediction Techniques	Amount data needed	Duration	Mathematical Skills
ARIMA	Data ≥ 50	Long-term	Strong
Regression	Data ≥ 10	Short-term	Middle
Holt's exponential	$10 \leq \text{Data} \leq 15$	Short-term	Middle
Grey system model	Data = 4	Short-term	Fundamentals

The Grey model requires basic skills of mathematics and a few amounts of data to analyze the system, as compared to other methods. The historical data of three sets for solar, wind, and load are introduced in this paper. Also, the model uses short-term forecasting because of short duration from one hour to 24 hours. With respect to criteria above, the Grey system model is selected for forecasting.

2.1.2 Mathematical Model of the Modified GM (1, 1)

The GM equation having N variables is known as GM (1, N). Assume $N = 1$, the GM with one variable is written as GM (1, 1). The differential equation of the GM (1, 1) model with parameters "a" and "b" is given by:

$$\frac{dP_k^{(1)}}{dt} + aP_k^{(1)} = b \quad (1)$$

The solution of equation (1) is given as:

$$\hat{P}_k^{(1)} = \left(P_1^{(0)} - \frac{b}{a} \right) e^{-a(k-1)} + \frac{b}{a} \quad (2)$$

For; $k \geq 2$

Let $\hat{P}^{(0)}$ be the power fitting/forecasting,

$$\hat{P}^{(0)} = (\hat{P}_1^{(1)}, \hat{P}_2^{(0)}, \hat{P}_3^{(0)}, \dots, P_{n+2}^{(0)}, P_m^{(0)}) \quad (3)$$

Where: $\hat{P}_1^{(1)}, \hat{P}_2^{(0)}, \hat{P}_3^{(0)}$ are the power fitting, while $P_{n+2}^{(0)}, P_m^{(0)}$, are the power predicting of the modified GM (1, 1) model.

Then, we have:

$$\hat{P}_k^{(0)} = (1 - e^a) \left(P_1^{(0)} - \frac{b}{a} \right) e^{-a(k-1)} \quad (4)$$

Where:

a & **b** are the average value of vectors of a_k and b_k

The Grey coefficient vectors are calculated as follows:

$$a_k = \log_e \left(\frac{P_{k-1}^{(0)}}{P_k^{(0)}} \right) \quad (5)$$

However, the background value of the modified GM (1, 1) is written as:

$$Z_k^{(1)} = \left(\frac{P_k^{(0)}}{\log_e(P_k^{(0)}) - \log_e(P_{k-1}^{(0)})} \right) + \left(\frac{P_1^{(0)} P_{k-1}^{(0)}}{P_{k-1}^{(0)} - P_k^{(0)}} \right) \quad (6)$$

And the vectors of the Grey control parameters are given as:

$$b_k = P_k^{(0)} + a_k Z_k^{(1)} \quad (7)$$

The mathematical of the modified GM (1, 1) model was further evaluated in the python program.

2.1.3 Simple Exponential Smoothing Method

The simple exponential smoothing equation is given in equation (8).

$$P_k''^{(0)} = \lambda P_k^{(0)} + (1 - \lambda) \hat{P}_k^{(0)} \quad (8)$$

Where: $0 < \lambda < 1$.

2.1.4 Mean Absolute Percentage Error (MAPE)

The MAPE evaluate the accuracy of power forecasting [16] and is calculated using equation (9):

$$MAPE = \frac{1}{m} \sum_{k=1}^m \frac{|P_k^{(0)} - P_{k+1}^{(0)}|}{P_k^{(0)}} \quad (9)$$

2.1.5 Historical Data

The historical data took from [17] and adapted to accomplish the purpose of the study. The actual power (in MW), produced and consumed against 24 hours duration from 00:00 hours to 23:30 hours as shown in Fig. 2.

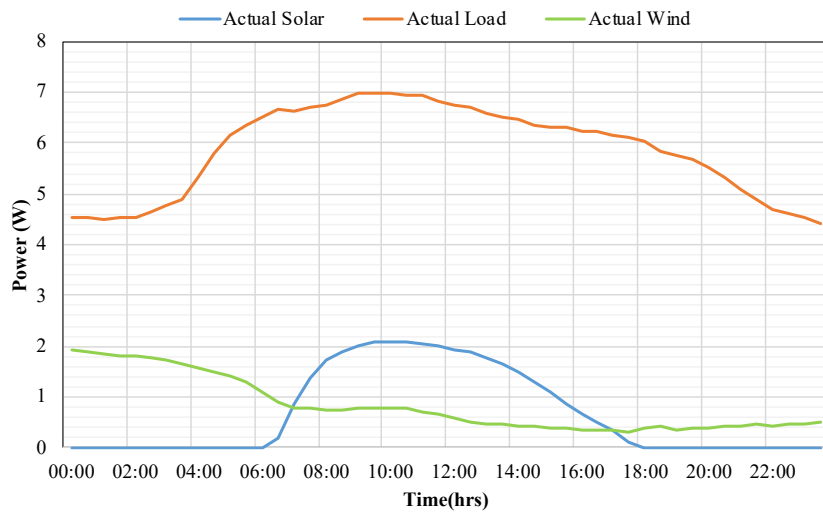


Fig. 2. Historical data for solar, wind, and load.

It is seen that the solar and wind generated minimum power around 1.2 kW and 0.32 MW. The maximum power generated were about 2.08 MW and 1.94 MW respectively. But the minimum and maximum power consumed was around 4.4 MW and 7 MW. This is unhealthy in operation of microgrid system since consumption is higher than the total generation. An extra is needed to balance mismatch. The purpose is not about to balance mismatch but to analyses line instability.

2.2. Line Instability

The line instability analysis is one of the areas in the power system used to analyze the system how far the line is close to voltage collapse. Consider the line with two buses in Fig. 3

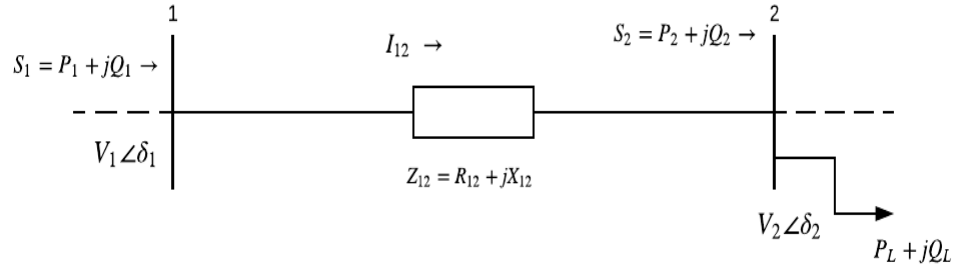


Fig. 3 Two bus networks [18].

Whereby;

δ = $\delta_1 - \delta_2$: Phase angle difference between bus 1 and 2.

Z_{12} = $R_{12} + j X_{12}$: Line impedance

Θ = Line impedance angle

From Fig. 3, the following are line instability indexes and their mathematical formulas:

2.2.1 Line Stability Factor (LQP)

The formula found in [19] and is given as follows in equation (10):

$$LQP_{12} = 4 \left(\frac{X_{12}}{V_1^2} \right) \left(Q_2 + \frac{X_{12} P_1^2}{V_1^2} \right) \quad (10)$$

2.2.2 Online Stability Index (LVSI)

The LVSI is determined by using equation (11):

$$LVSI_{12} = \frac{4R_{12}P_2}{[V_1 \cos(\theta - \delta)]^2} \quad (11)$$

2.2.3 Line Stability Index (Lmn)

Researcher [20] wrote that Lmn formula is evaluated in equation (12):

$$Lmn_{12} = \frac{4X_{12}Q_2}{[V_1 \sin(\theta - \delta)]^2} \quad (12)$$

2.2.4 Fast Voltage Stability Index (FVSI)

Reference [21] wrote that the FVSI equation is presented using equation (13). The expression of FVSI is given by:

$$FVSI_{12} = \frac{4Z_{12}^2 Q_2}{V_1^2 X_{12}} \quad (13)$$

Equations 10, 11, 12, and 13 indicate that the FVSI and L_{mn} are directly relative to reactive power. But, the LQP includes active and reactive power of the line, and LSVI contains active power only.

The LQP has better performance than the other indexes [22] because it consists of active and reactive power of the line as a result of different power factors. Thus, this paper considers applying LQP to estimate line instability.

However, the determination of the line instability is based on the power flow results. With the line stability factor is near to one, the microgrid is said to be close to instability [23].

2.3. Power Flow Analysis

This method used to analyze and ensure power is transferred from generation sources to consumers. The power flow calculates the voltage, current, active, and reactive power in a network under a load condition. The power flow was executed using the Newton-Raphson technique in MATLAB.

Newton-Raphson method is one of the techniques used to determine a set of non-linear equations with the same number of unknowns. Assume that i and j are the bus indexes, where $i, j = 1$ to N .

N is the number of buses. The standard form of the node equation is given as follows:

$$I_i = \sum_{j \in i} V_i Y_{ij} \quad (14)$$

where, $j \in i$, denotes the bus j is connected to bus i

For $j = i$

$$H_{ij} = \sum_{j \in i, j \neq i} V_j (G_{ij} \sin \theta_{ij} - B_{ij} \cos \theta_{ij}) \quad (15)$$

$$N_{ii} = -V_i \sum_{\substack{j \in i \\ j \neq i}} V_j (G_{ij} \cos \theta_{ij} + B_{ij} \sin \theta_{ij}) - 2V_i^2 G_{ij} \quad (16)$$

$$J_{ii} = -V_i \sum_{\substack{j \in i \\ j \neq i}} V_j (G_{ij} \cos \theta_{ij} + B_{ij} \sin \theta_{ij}) \quad (17)$$

$$L_{ii} = -V_i \sum_{j \in i, j \neq i} V_j (G_{ij} \sin \theta_{ij} - B_{ij} \cos \theta_{ij}) + 2V_i^2 B_{ij} \quad (18)$$

For $j \neq i$

$$H_{ij} = -V_i V_j (G_{ij} \sin \theta_{ij} - B_{ij} \cos \theta_{ij}) \quad (19)$$

$$N_{ii} = -V_i V_j (G_{ij} \cos \theta_{ij} + B_{ij} \sin \theta_{ij}) \quad (20)$$

$$J_{ii} = -V_i V_j (G_{ij} \cos \theta_{ij} + B_{ij} \sin \theta_{ij}) \quad (21)$$

$$L_{ii} = -V_i V_j (G_{ij} \sin \theta_{ij} - B_{ij} \cos \theta_{ij}) \quad (22)$$

The equation of the Newton-Raphson power flow is given by:

$$\begin{bmatrix} \Delta P \\ \Delta Q \end{bmatrix} = \begin{bmatrix} H & N \\ J & L \end{bmatrix} = \begin{bmatrix} \Delta \theta \\ \Delta V / V \end{bmatrix} \quad (23)$$

Where H , N , J , and L are Jacobian elements.

$$\begin{aligned} H_{ij} &= \frac{\partial \Delta P_i}{\partial \Delta \theta_j}, & N_{ij} &= \frac{\partial \Delta P_i}{\partial \Delta V_j} V_j \\ J_{ij} &= \frac{\partial \Delta Q_i}{\partial \Delta \theta_j}, & L_{ij} &= \frac{\partial \Delta Q_i}{\partial \Delta V_j} V_j \end{aligned}$$

The following were stages used to carry out power flow calculations:

- (1) State the values of the parameters for power system components
- (2) State locations and values for the loads in the power system
- (3) State specifications for the generations in the network
- (4) Create the mathematical model
- (5) Determine the voltage profile in the model equations
- (6) Determine the power flow and losses in the model equations
- (7) Verification for constraint violations.

2.3.1 IEE 30 Bus Test System

Assume that the microgrid is operating in an island mode and the IEEE 30 bus as a base test case. The details of the IEEE 30 bus test system are avail in [24]. The single line IEEE 30 bus test system is shown in Fig. 4. The IEEE 30 bus standard test system has the following connected components:

Number of generators	=	6
Number of loads	=	20
Slack bus number	=	1
number lines	=	41
base voltage	=	22 kV
Base power	=	100 MVA.

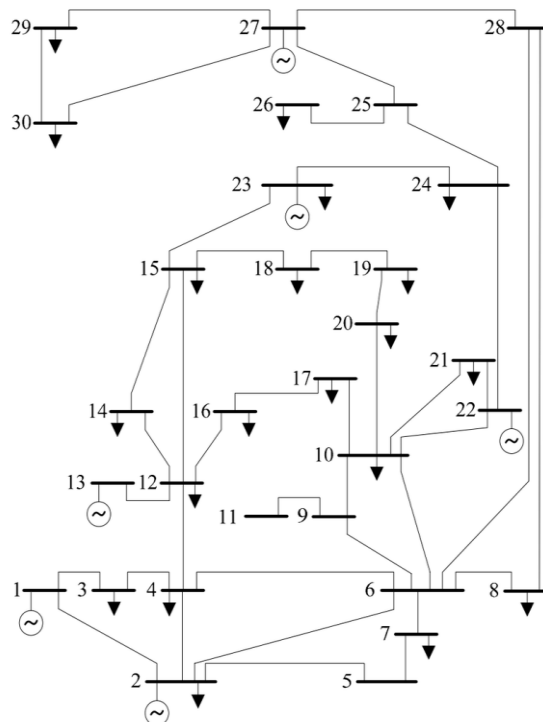


Fig. 4 Single Line diagram of IEEE 30 [25].

The overall steps of the methodology are summarized in the proposed flow chart in Fig. 5

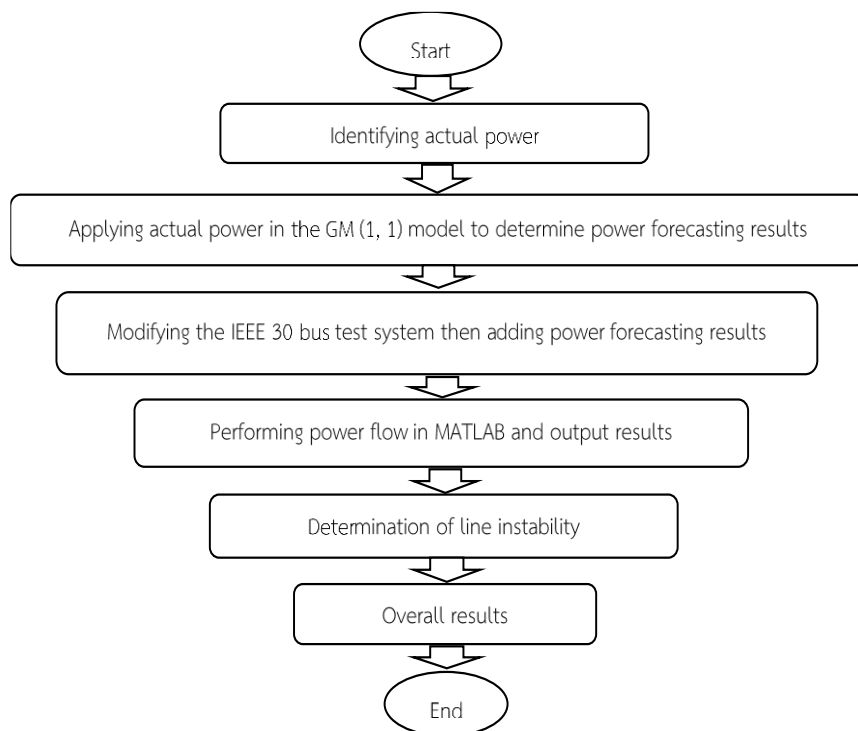


Fig. 5. Proposed Methodology Flow Chart.

3. Results and Discussions

The results detailed in three sections: electric power forecasting, power flow analysis, and line instability.

3.1. Power Forecasting Results

The results exhibited that the actual power is very close to the power forecasting results. The wind power showed downward trends, whereas solar power gave both downward and upward inclinations. The load demands experienced some fluctuations, as illustrated in Fig. 6.

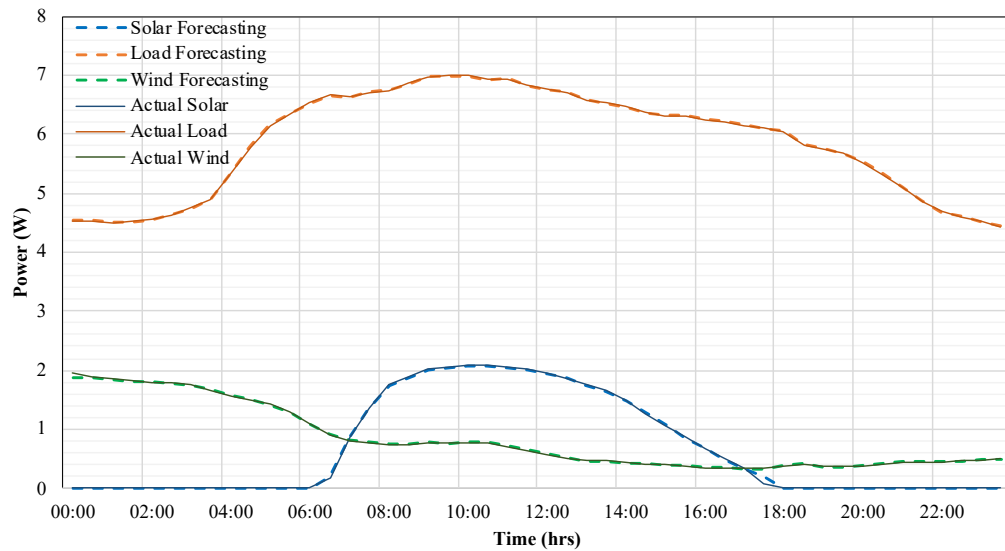


Fig. 6. Power Forecasting Results.

The maximum and minimum power forecasting consumed was about 6.9 MW and 4.4 MW, whereas the maximum and minimum power generation forecasting were around 2.05 MW and 0.99 kW for solar power and 0.32 MW and 1.8 MW for wind power. Still, the power consumed forecasting was higher than the power prediction for generation (solar and wind). This not healthy in operation and control of the system.

3.1.1 Mean Absolute Percentage Error (MAPE)

The MAPE of the load demands, solar power, and wind power are presented in Table 2. The MAPE for solar, wind and load were 0.778%, 0.302%, and 0.024% accordingly. These MAPE were obtained after an exponential smoothing method used together with the modified GM (1, 1) model.

Table 2 MAPE Results.

	Load Demands	Solar Power Output	Wind Power Output
MAPE	0.024	0.778	0.302

3.2. Proposed System and Power Flow Analysis

Before the power flow, the IEEE 30 bus system was altered to make sure the test system data are within the microgrid standard. Also, the base power was modified to 10 MVA, and the base voltage was limited to 1.0 p.u.

Now, the eight highest values of power forecasting of load demand and generation (solar plus wind) were chosen and presented randomly in the modified IEEE 30 test base case. The eight values of power forecasting for the load demands were 6.75 MW, 6.82 MW, 6.85 MW, 6.93 MW, 6.94 MW, 6.98 MW, 6.99 MW, and 7 MW whereas for generations (solar plus wind) were 3.45 MW, 3.6 MW, 3.74 MW, 3.78 MW, 3.84 MW, 3.87 MW, 3.9 MW, and 3.94 MW.

For the load demands, the highest value of power forecasting was located at bus numbers 6, 9, 11, 13, 22, 25, 27, and 28 while for the generation were set at bus number 6, 9, 11, 16, 22, 24, 26, and 30.

After introducing the power forecasting in the modified IEEE 30 bus test system, then it was assumed that the proposed system was for a day-ahead. Thus, the power flow was studied based on the proposed system. The power flow results of the proposed system showed that the total power generated and consumed were 75.403 MW and 69.362 MW, while the total power losses were 6.041 MW.

3.3. Line Instability Results

The results obtained from the power flow were used to determine the line instability using equation (10). The results of the line stability factor represented in Table 2.

From table 2, it shows that the line 27-28 was considered to be the most critical line to bus 27 because of a high instability factor of 0.963 whereas, the line 6-8 was the least critical line to bus to 6. Besides that, the line 25-26 is the second most crucial line to bus 26 with a stability factor of 0.759, while the third most critical line to bus 4 is line 2-4 with stability factor 0.568 subsequently.

When the line instability factor is near to one, it indicates that the line is very close to the point of voltage collapse. For that reason, the precaution must be taken by the utility operator before a next day operation control and planning to operate the microgrid successfully.

Table 2 Line Instability Results.

Bus	Bus	Instability	Critical	Bus	Bus	Instability	Critical		
No	From	To	Factor	line	No	From	To	Factor	line
2	2	4	0.568	3	12	12	13	0.139	7
4	4	12	0.233	5	24	24	25	0.172	6
6	6	8	0.111	10	25	25	26	0.759	2
8	8	28	0.120	8		25	27	0.114	9
9	9	11	0.264	4	28	28	27	0.963	1

4. Conclusion

By taking into account the next day operation of the microgrid, this paper was positively presented an analysis of the line instability in microgrid by application of power forecasting approach.

The electric power forecasting was studied using the modified GM (1,1) model then combined with a simple exponential smoothing. The results showed that high accuracy of forecasting when the

modified GM (1, 1) model was used together with a simple exponential smoothing method. The overall MAPE was less than 1%.

Apart from that, the actual minimum and maximum power consumed is about 4.4 MW and 7 MW respectively while the actual minimum and maximum power generated (solar plus wind) were about 0.375 MW and 4.02 MW.

The forecasting minimum and maximum consumed were around 4.4 MW and 6.9 MW. Whereas, the forecasting minimum and maximum power generated (solar plus wind) were about 2.12 MW and 3.04 MW. The variation of power generated in microgrid created such unhealthy situation which lead researcher to analyze line instability.

The power forecasting was attached in the modified IEEE 30 bus test system, and the power flow was carried out using the Newton-Raphson method in MATLAB, and lastly, the line instability was examined based on the power flow results of the proposed system.

From the instability results point of view, it revealed that the most critical line was at line 27-28 with an instability factor of 0.963, whereas the least critical line was at line 6-8 with an instability factor of 0.111. Overall, it revealed that the 24-hours power forecasting helps to understand day-ahead operation control and planning in the microgrid.

Acknowledgments

The author would like to thank the Suranaree University of Technology and Rajamangala University of Technology Rattanakosin for supporting this research.

Nomenclatures

$P_1 : Q_1$	=	Active and reactive power flow at the sending bus 1
$P_2 : Q_2$	=	Active and reactive power flow entering the receiving bus 2
$S_1 : S_2$	=	Apparent power at the sending and receiving buses 1, 2
$P_k^{(0)}$	=	Actual power
I_i	=	Current at bus i
I_{ij}	=	Current flow in the line
$\partial P_k^{(1)} / \partial t$	=	Estimated energy used at time t
$P_k^{(1)}$	=	Estimated power used at time t
a	=	Grey coefficient
b	=	Grey control parameter.
$P_1^{(0)}$	=	Initial value of power for $t = 1$ and for a given series to be modeled.
$P_k^{(0)}$	=	Previous actual power
δ_1	=	Phase angle at the sending bus 1
δ_2	=	Phase angle at the receiving bus 2
R_{ij}	=	Resistance of the line
λ	=	Smooth parameter

$$\begin{aligned}V_1 &= \text{Voltage at the sending bus 1} \\V_2 &= \text{Voltage at the receiving bus 2}\end{aligned}$$

References

- [1] Joseph, R. & Marungsri, B. (2019, September 23-24). *Evaluation of line voltage stability index in micro-grid with or without BESS*. PEA Conference and Innovation, Bangkok, Thailand.
- [2] Subramani, C., Subhransu, S. D., Bhaskar, A. M. & Jagdeshkumar, M. (2009). Simulation technique for voltage stability analysis and contingency ranking in power systems. *International Journal of Recent Trends in Engineering*, 2(5), 263-267.
- [3] Thasnas, N & Siritaratiwat, A. (2019). Implementation of static line voltage stability indices for improved static voltage stability margin. *Journal of Electrical and Computer Engineering*, from <https://doi.org/10.1155/2019/2609235>
- [4] Goh, H. H., Chua, S. S., Lee, W. S., Kok, C. B., Goh, C. K. & Teo, K. T. K. (2015). Evaluation for voltage stability indices in power system using artificial neural network. *Procedia Engineering*, 118, 1127-1136.
- [5] Lotufo, P. D. A & Minussi, R. C. (2002, August 28 – September 2). *Electric power system load forecasting: A survey*. IEEE - International Conference on Power Technology, Budapest, Hungary.
- [6] Piao, M., Lee, G. H, Park, H. J. & Ryu, H. K. (2008, September 15-18). *Application of classification methods for forecasting mid-term power load patterns*. 4th International Conference on Intelligent Computing, Shanghai, China.
- [7] Deng, J. (1989). Introduction to Grey System Theory. *Journal of Grey System*, 1, 1-24.
- [8] Huang, Y., Fang, W., & Fan, Z. (2011, January 8-9). *Application research of improved Grey Forecasting Model in load forecasting*, International Conference on Intelligent Computing and Information Science, Chongqing, China.
- [9] Wang, H. C & Phan, T. V. (2014). An improvement of the accuracy of Grey Forecasting Model for cargo throughput in international commercial ports of Kaohsiung. *WSEAS Transactions on Business and Economics*, 11, 322-327.
- [10] Kayacan, E., Ulutas, B. & Kaynak, O. (2010). Grey system theory-based models in time series prediction. *Expert Systems with Applications*, 37, 1784-1789.
- [11] Oukenou, A. and Sandali, A. (2019). An improved reactive line index for line ranking and voltage collapse prediction in transmission power system. *Journal of Electrical Systems*, 15(3), 480 – 498.
- [12] Reis, C., Andrade, A. & Maciel, F. P. (2009, March 18 – 20). *Line Stability Indices for Voltage Collapse Prediction*. International Conference on Power Engineering, Energy, and Electrical Drives, Lisbon, Portugal.
- [13] Choudekar, P., Asija, D. & Ruchira, (2017). *Prediction of voltage collapse in power system using voltage stability indices*. Proceeding of International Conference on Intelligent Communication, Control and Devices, Dehradun, India.
- [14] Hsu, C. & Chen, C. (2003). Application of improved Grey Prediction Model for power demand forecasting. *Energy Conversion and Management*, 44(12), 2241-2249.
- [15] Wang, Y., Liu, Q., Tang, J., Cao, W. & Li, X. (2014). Optimization approach of background value and initial item for improving prediction precision of GM (1, 1) model. *Journal of Systems Engineering and Electronics*, 25(1), 77-82.
- [16] Sobhani, M., Campbell, A., Sangamwar, S., Li, C. & Hong, T. (2019). Combine weather stations for electric load forecasting, *Energies*, 12(8), 1-11.
- [17] Neon Neue Energieökonomik GmbH. (n.d.). *Data Platform*. Retrieved August 20, 2019, from https://data.open-power-system-data.org/time_series/

- [18] Eminoglu, U. & Hocaoglu, M. H. (2007, September 4 - 6). *A voltage stability index for radial distribution networks*. 42nd International Universities Power Engineering Conference, Brighton, UK
- [19] Mohamed, A & Jasmon. G. B. (2007). A new clustering technique for power system stability analysis. *Journal of Electrical Machines and Power Systems*, 23(4), 389-403.
- [20] Moghavemmi, M. & Omar, F. M. (1998). A technique for contingency monitoring and voltage collapse prediction. *IET - Proceedings Generation Transmission and Distribution*, 145(6), 634-640.
- [21] Musirin, I & Abdul Rahman, T. K. (2002). Estimating maximum load ability for weak bus identification using FVSI. *Power Engineering Review*, 12(11), 50-52.
- [22] Zhang, X., & Wong, C. K. (2011, October 3-5). *Comparison of voltage stability indexes considering dynamic load*. Electrical Power and Energy Conference, Winnipeg, MB, Canada.
- [23] Subramani, C., Subhransu, S. D., Kumar, V. & Harish, K. (2012). Implementation of line stability index for contingency analysis and screening in power systems. *Journal of Computer Science*, 8(4), 585-590.
- [24] Saadat, H. (1999). *Power System Analysis*, New York, USA: McGraw-Hill.
- [25] Wordpress.com. (n.d.). *World Electrical Engineering*. Retrieved May 20, 2020, from <https://kalyan07.wordpress.com/2014/1/>